International Conference on Space Optics—ICSO 2022

Dubrovnik, Croatia

3–7 October 2022

Edited by Kyriaki Minoglou, Nikos Karafolas, and Bruno Cugny,

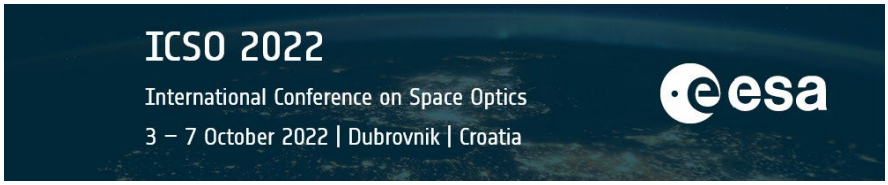

Laser-induced thermal effects in optical interference coatings: Temperature and thermal radiation

International Conference on Space Optics — ICSO 2022, edited by Kyriaki Minoglou, Nikos Karafolas, Bruno Cugny, Proc. of SPIE Vol. 12777, 127775H · © 2023 ESA and CNES · 0277-786X · doi: 10.1117/12.2691026

Laser-induced thermal effects in optical interference coatings: Temperature and thermal radiation

Paul Rouquette[1,2], Claude Amra[1], Myriam Zerrad[1], Hélène Krol[2], Catherine Grèzes-Besset[2], Karine Mathieu[3]
[1]*Aix Marseille Univ, CNRS, Centrale Marseille, Institut Fresnel, Faculté des Sciences - Campus Saint Jérôme, Avenue Escadrille Normandie-Niemen, 13397 Marseille, France*
[2]*CILAS ArianeGroup, 600 avenue de La Roche Fourcade, Pôle Alpha-Sud, 13400 Aubagne*
[3]*CNES, 18 avenue Edouard Belin 31401 Toulouse, France*
Paul.rouquette@fresnel.fr, claude.amra@fresnel.fr

ABSTRACT

We present an original modelling of photo-induced temperature and thermal radiation in optical coatings submitted to arbitrary spatio-temporal illumination. Numerical results are given at different temporal and spatial scales. The question of emissivity engineering is addressed.

1. INTRODUCTION

Optical interference coatings are commonly used for a large panel of optical components for Space applications. Once submitted to a laser illumination, a small amount of the laser energy is absorbed by the filter materials, which induces a rising temperature inside the component and therefore a change in its thermal radiation. These laser-induced thermal effects are a major issue in the field of Space communication or defense as they can be responsible for many problems ranging from degradation of optical performance to irreversible damage. Furthermore, they are the basis of the various processes for characterizing the absorption of filters such as photo-thermal deflection, common path interferometry or lock-in thermography.

Huge efforts, both theoretical and experimental, have been made to describe and predict these phenomena. Most of the work [1–6] focuses on the rising temperature that can damage the component [7,8]. Existing models are mostly numerical and based on solving the heat equation. Analytical models exist, in the sense that they do not rely exclusively on numerical methods, but they are generally limited. They use a partial description of the thermal source [9,10] or consider continuous or infinitely short laser regimes [11,12]. Regarding thermal radiation, its modelling is often reduced to an emissivity calculation in connection with Kirchhoff's law, which stipulates its equality with absorption. However, this method proves insufficient when one wants to go further into the details of the thermal process balance (evanescent waves, guided modes by coupling, transient regimes).

In this context, we propose theoretical models to accurately predict photo-induced thermal phenomena (rising temperature and thermal radiation) in optical thin films under arbitrary illumination regimes (pulsed, clocked, continuous). The method of resolution is based on work related to luminescent microcavities [13,14] and scattering of light in filters [15,16].

In order to obtain the laser induced temperature, the heat equation with the absorption density of the coatings for the source term is solved with an original analytical method based on the Fourier Transform and an analogy between optical propagation and heat diffusion [17]. This allows us not only to obtain the spatial and temporal evolution of the temperature as a function of laser and components parameters, but also to determine laws to predict the maximum temperature elevation, which is a major information for the user and enables to study the nature, thermal or dielectric, of the laser-induced damage threshold.

To study thermal radiation, an electromagnetic approach is used to model the thermal agitation of charged particles by electric current densities [18–21]. These currents, which are related to the temperature elevation by statistical tools, are then introduced in Maxwell's equations to get the spectral, temporal, and angular patterns of the thermal radiation of arbitrary optical filters submitted to different optical sources.

To summarize, the main steps in the modelling of photo-induced thermal phenomena are illustrated by the three diagrams in Figure 1.1. The diagram shows a two-dimensional optical interference filter with interfaces between layers perpendicular to the z axis. The x axis represents the transverse dimension. This component is illuminated by spatially and temporally variable optical illumination, which induces a volume density of absorption in the layers, the source of photo-induced thermal effects (step 1). An energy balance between this absorption and the thermal transfer modes (conduction only) then allows the temperature rise in the component to be predicted (step 2). The thermal agitation of the particles is finally modelled by volume densities of electric and magnetic currents that generate radiation propagating in the extreme media (step 3).

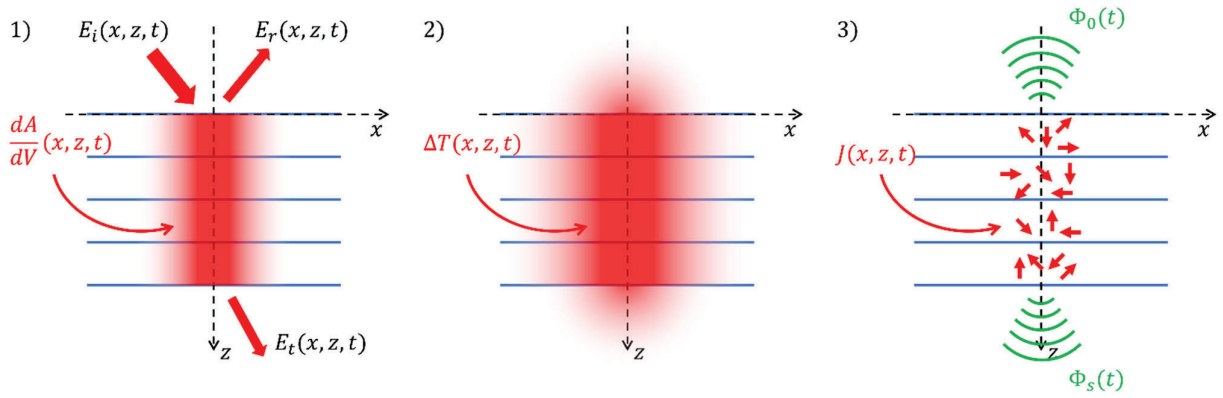

Figure 1.1: The main steps in the modelling of laser-induced thermal phenomena in optical interference coatings. E_i,E_r and E_t represents the incident, reflected and transmitted electric field respectively. The bulk absorption density is denoted by dA/dV and induces a rising temperature $\boldsymbol{\Delta T}$. Electric currents are written $\boldsymbol{J}$ and produce a radiated flux $\boldsymbol{\Phi_0}$ in superstrate and $\boldsymbol{\Phi_s}$ in substrate. The power carried by guided modes is written $\boldsymbol{F_g^m}$.

2. LASER INDUCED TEMPERATURE IN OPTICAL INTERFERENCE FILTERS

The object of study is a multilayer stack composed of p dielectric layers deposited on a glass substrate. The substrate is denoted by s and the superstrate (air) is the medium 0. For each layer i, the complex optical index is denoted $n_i = n_i' + jn_i''$ and the thickness e_i. A schematic of the component is provided in Figure 2.1. The normal direction is the z axis.

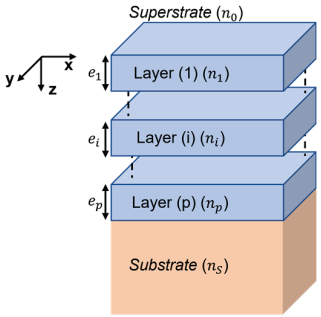

Figure 2.1: geometry of an optical interference filter (see text).

To obtain the rising temperature in optical interference coatings, it is sufficient to carry out an energy balance between the absorption volume density and the heat transfer modes. If the convection and thermal radiation are neglected, this reduces to the classical heat equation which can be written, in every layer of the component, as:

$$\Delta T_i(\vec{\rho},t) - \frac{1}{a_i}\frac{\partial T_i}{\partial t}(\vec{\rho},t) = -\frac{1}{b_i}S_i(\vec{\rho},t) \qquad (1)$$

where (a_i, b_i) are respectively the thermal diffusivity ($m^2.s^{-1}$) and thermal conductivity ($W.m^{-1}.K^{-1}$) of layer $n°i$. $T_i(\vec{\rho},t)$ is the temperature field at time t and at point $\vec{\rho}$ in the layer. The thermal source S_i, which is the absorption volume density in the layer, is related to the laser parameters and the optical indices of the component.

Equation (1) is solved by using an analogy between optical propagation in metallic media and heat diffusion [17]. To do so, equation (1) is expressed in the Fourier plane by using a double Fourier Transform with respect to the time and the transverse space variable. A complete description of the resolution method can be found in [22].

For arbitrary stack and optical illumination, the model provides a temperature field that depends on the time variable t and the space variable $\vec{\rho} = (x, y, z)$. To give an example, a Fabry-Perot filter with a central wavelength of 1064 nm is studied in Figure 2.2. The formula of the component is: $Air/H(LH)^2 6L(HL)^2 H/BK7$ where H refers to a high index quarter wave layer, composed of Nb_2O_5, and L to a low index quarter wave layer, composed of SiO_2. The BK7 substrate is assumed to be non-absorbent. The thermal and optical parameters of the materials are summarized in Table 1.

Table 1: Thermal and optical parameters used for numerical calculations

Materials	SiO_2	Nb_2O_5	Air	Substrate: BK7
Refractive index @ 1 µm	$1.45+10^{-5}$j	$2.25+10^{-5}$j	1	1.52
Thermal conductivity (W/m/K)	0.5	1.0	$2.5*10^{-2}$	1.14
Thermal diffusivity (m²/s)	$1.84*10^{-7}$	$4.3*10^{-7}$	$2.05*10^{-5}$	$6.2*10^{-7}$

This Fabry-Perot filter is submitted to a laser illumination with an energy of 1 mJ, at normal incidence and with a central wavelength of 1064 nm. The spot radius, defined at 1/e², is 100 µm.

In Figure 2.2 a) the rising temperature ΔT is plotted as a function of the height z in the component, for two pulse duration (ns in blue and ms in red). The altitude $z = 0$ corresponds to the position of the top surface. For both regimes (ns and ms), the temperature elevation ΔT is considered at the instant when it is maximum. This distribution may be compared in Figure 2.2 b) with that of the normalized electric field inside the component. As previously shown in [2,5,6], it may be noted that for short duration pulses (< ns), the temperature field has a distribution similar to that of the stationary electric field, which is not the case in the ms regime in which it is quasi-constant. This result is due overall to the thermal diffusion length [7]:

$$L_d = 2\sqrt{a\tau} \quad (2)$$

where τ is the width at 1/e² of the laser pulse which is assumed to be Gaussian, and a the diffusivity of the medium in question.

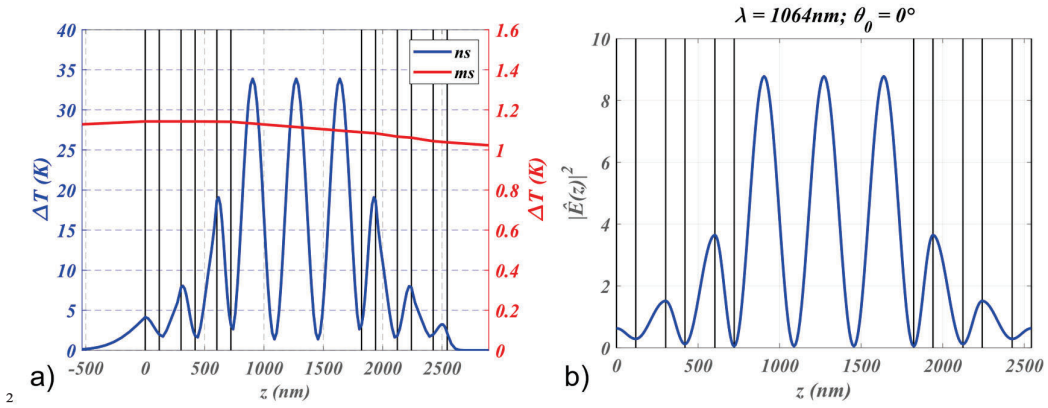

Figure 2.2: Profiles of temperature (a) and of the square of the electric field normalized by the incident field (b) in the thickness of the multi-dielectric component, calculated for 2 different laser regimes (ps and ms).

From a practical viewpoint, information which is essential for the user relates to the maximum temperature elevation obtained in the component as a function of the energy, the pulse duration, the illuminated surface and the imaginary index of the material. It is in fact these data which make it possible to grasp the importance of the photo-induced thermal phenomena which we are attempting to summarize and simplify. Results will be found in [23].

Finally, our model allows us to compare the thermal and electrical damage thresholds as a function of the illumination parameters and the imaginary indices of the thin-film materials. Very many works have been devoted to the laser damage of components under flux [2,7,8,24–27]. It is known that for short pulse durations (typically less than one ns), the damage

process is not thermal but resembles the concept of dielectric breakdown caused by the high value of the electromagnetic field. Thus, it is common practice to define for these short pulses a laser damage threshold, or electromagnetic damage threshold, as a reminder that it is related to the value of the optical field (rather than the temperature). This threshold naturally depends on the materials and technologies used for manufacturing the thin films, the formula of the component, the illumination conditions and also on the nature and the density of defects in the components.

This damage issue is similar for longer pulses, except that the damage process is thermal in nature (the temperature in the component approaches the melting temperature T_f). In this context, it is helpful to consider another (thermal) damage threshold, which represents the laser fluence F that must not be exceeded so that the temperature in the component does not reach the melting temperature of the materials. The calculation of this threshold refers to a temperature calculation and our formalism can thus be used [23].

3. LASER INDUCED THERMAL RADIATION

We now turn our attention to the thermal radiation induced by the rising temperature studied in the previous section. To do so, we rely on works on statistical physics which enable to model thermal radiation in an electromagnetic way. According to [18–21], the classical way to model it at the nanoscale is to consider an electrical current density, written $\vec{J}_e(\vec{r},z,t)$, which represents the random thermal movement of charged particles. For a local isotropic medium at thermal equilibrium, the spatial correlation function of the current at two different locations can be linked the temperature as follows:

$$\langle \tilde{J}_{m,e}(\vec{\mathrm{r}},z,f)\tilde{J}^{*}_{n,e}(\vec{\mathrm{r}}',z',f)\rangle = 4\pi\epsilon''(f)\Theta(f,T)\delta_{nm}\delta(\vec{\mathrm{r}}-\vec{\mathrm{r}}')\delta(z-z') \quad (3)$$

where $\langle . \rangle$ is a statistical average, $m,n \in \{x,y,z\}$ are the coordinates of the current density, ϵ'' is the imaginary part of the dielectric permittivity of the medium, $\Theta(f,T) = hf/(e^{hf/k_BT}-1)$ is the mean energy of Planck's oscillator at the frequency f and temperature T in thermal equilibrium, δ_{nm} is the Kronecker symbol and $\tilde{J}_{m,e}(\vec{\mathrm{r}},z,f) = \int J_{m,e}(\vec{\mathrm{r}},z,f)e^{j2\pi ft}dt$ is the Fourier Transform of the current density versus the time variable. This current density is then inserted into Maxwell's equation to get the electromagnetic field induced by the temperature of the medium, that is, the thermal radiation. Using this technique, Francoeur and al [28] calculated the thermal radiation flux of a multilayer structure where each layer is in thermal equilibrium and thus has its own current density.

To satisfy the thermal equilibrium hypothesis in our interference coatings, the temperature elevation of section 2 is discretized in time and space. We obtain a series of multilayer structures where each layer has a constant temperature over a given period of time. We place ourselves in the situation described in [28,29] where the authors make the use of Dyadic Green functions to solve the problem. Here, we choose to rely on the works related to luminescent micro-cavities [13,14] and scattering of light in filters [15,16] in order to use theoretical and numerical tools that were previously developed. More details on the calculation steps can be found in [22].

To illustrate the modelling, the laser induced thermal radiation of a multi-dielectric mirror is studied in Figure 3.1. The component is a miror, centered at 1064 nm, of formula $(HL)^4H$ deposited on a BK7 substrate assumed to be non absorbent. The thermal and optical parameters of the materials are the ones of Table 1. This mirror is submitted to a ns pulse laser with an energy of 10 mJ, a spot radius of 100 µm and a central wavelength of 1064 nm. Optical index dispersion is not considered in the calculation.

The radiative spectral intensity [21] of the miror in the superstrate is shown against the time in Figure 3.1 a). This intensity is plotted at its maximum, thus at normal incidence ($\theta_0 = 0°$) and in the mid infrared region ($\lambda = 7.7\mu m$). Figure 3.1 b) plots the spectral intensity as a function of the emission wavelength, still at $\theta_0 = 0°$. Figure 3.1 c) plots the spectral intensity as a function of the angle of emission in the superstrate at $\lambda = 7.7\mu m$. The blue curve represents the radiative intensity at ambient temperature chosen here at 20°C, shown by a blue dot on the temporal curve given in Figure 3.1 a). The red curve corresponds to the instant at which the intensity is a maximum, shown by the red dot on the temporal curve in Figure 3.1 a). Note that for this calculation, the dispersion of the optical indices is not taken into account (despite the spectral range), even though these dielectric materials become absorbent in the mid infra-red (MIR); consequently, radiation levels must be higher in the MIR.

From Figure 3.1 we can deduce that, for temperature closed to 20°C, optical thin films behave as blackbody except for the low signal levels due to the low absorption of the materials. In order to observe the effect of the filter formula on the blackbody radiation, we must either use a mirror centered about 8 µm, or increase the temperature elevation to shift the radiation to shorter wavelengths (1064 nm). More details will be found in [30].

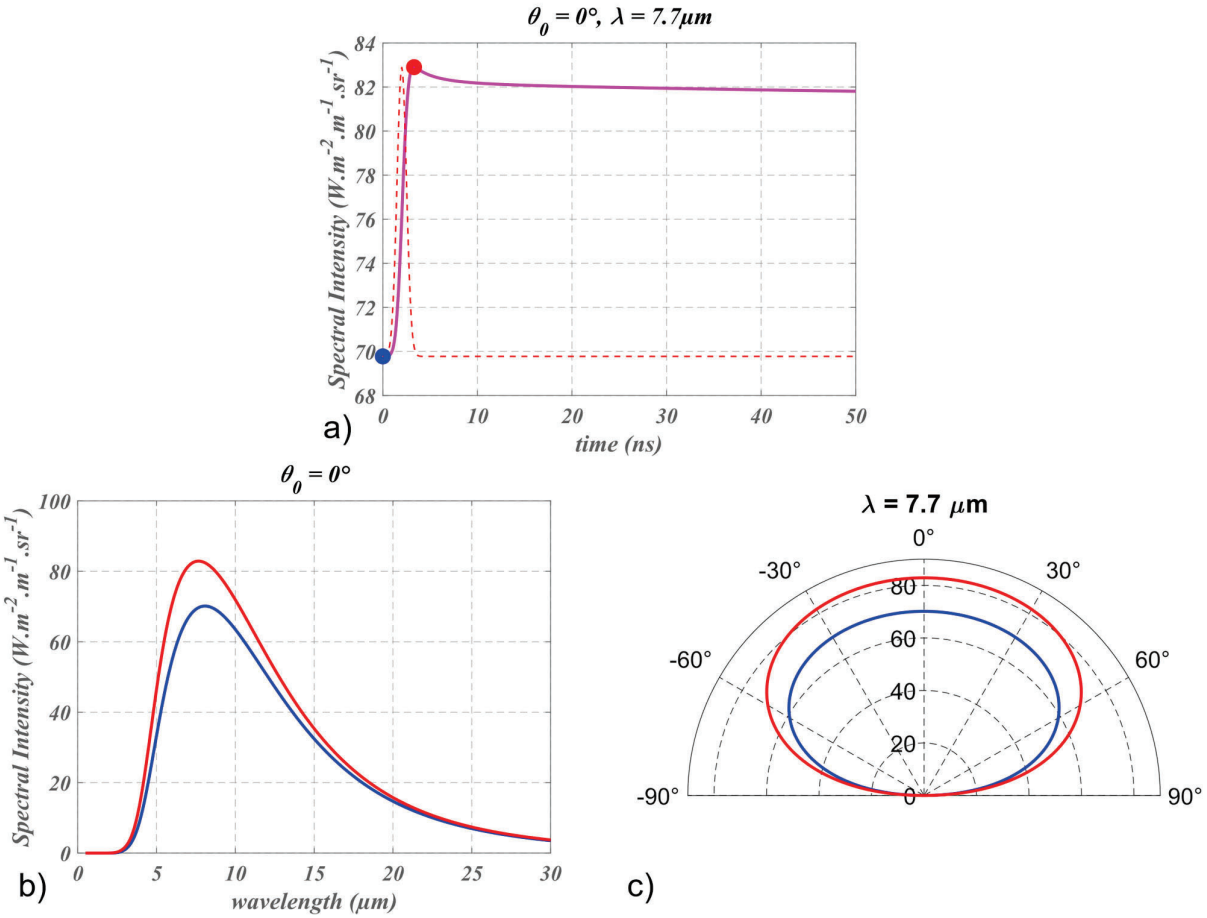

Figure 3.1: Spectral intensity of the thermal radiation of a multi-dielectric mirror subjected to a 10mJ ns pulsed laser. a) temporal evolution at normal emission angle and $\lambda = 7.7\mu m$. b) spectral variation at normal emission angle. c) angular variation at $\lambda = 7.7\mu m$. The red and blue curves are calculated respectively at the instants given by the red and blue dots of figure a).

4. CONCLUSION

The photo-induced temperature and thermal radiation of optical interference have been modelized in a very precise way. The models enable to predict the temporal and spatial variation of these two quantities for arbitrary multilayer stack subjected to arbitrary illumination.

We believe this work may be very useful for Space applications as it can predict the levels of thermal radiation and those of thermal damage threshold. Furthermore, since the modelization relies on a thin film multilayer approach, it could pave the way of tailoring thermal radiation over large or narrow wavelength bandwidths. This could lead to the fabrication of components with outstanding energy-saving characteristics such as selective solar absorbers [31] or radiative coolers [32].

REFERENCES

1. M. Mansuripur, G. A. N. Connell, and J. W. Goodman, "Laser-induced local heating of multilayers," Appl. Opt. **21**, 1106–1114 (1982).
2. H. Hu, Z. Fan, and F. Luo, "Laser-induced damage of a 1064-nm ZnS/MgF_2 narrow-band interference filter," Appl. Opt. **40**, 1950–1956 (2001).
3. G. Chen, Y. Chen, J. Lu, Z. Shen, and X. Ni, "Analysis of laser induced thermal mechanical relationship of HfO2/SiO2 high reflective optical thin film at 1064 nm," Chin. Opt. Lett. **7**, 601–604 (2009).

4. B. Wang, Y. Qin, X. Ni, Z. Shen, and J. Lu, "Effect of defects on long-pulse laser-induced damage of two kinds of optical thin films," Appl. Opt. **49**, 5537 (2010).
5. B. Wang, X. Wang, Y. Qin, X. Ni, Z. Shen, and J. Lu, "Temperature field analysis of optical coatings induced by millisecond and nanosecond lasers," Opt. Appl. **42**, 783–793 (2012).
6. H. Li, Z. Shen, and X. Ni, "Temperature field analysis of high reflection film induced by long-pulse and short-pulse lasers under different irradiation angles," Optik **126**, 4254–4258 (2015).
7. R. M. Wood, *Laser-Induced Damage of Optical Materials*, Series in Optics and Optoelectronics (Institute of Physics, 2003).
8. D. Ristau, *Laser-Induced Damage in Optical Materials* (CRC Press, 2015).
9. A. Salazar, R. Fuente, E. Apiñaniz, A. Mendioroz, and R. Celorrio, "Simultaneous measurement of thermal diffusivity and optical absorption coefficient using photothermal radiometry. II Multilayered solids," J. Appl. Phys. **110**, 033516 (2011).
10. R. Fuente, E. Apiñaniz, A. Mendioroz, and A. Salazar, "Simultaneous measurement of thermal diffusivity and optical absorption coefficient using photothermal radiometry. I. Homogeneous solids," J. Appl. Phys. **110**, 033515 (2011).
11. A. Salazar, A. Mendioroz, and A. Oleaga, "Flying spot thermography: Quantitative assessment of thermal diffusivity and crack width," J. Appl. Phys. **127**, 131101 (2020).
12. C. Wei, "Study of thermal behaviors in CO2 laser irradiated glass," Opt. Eng. **44**, 044202 (2005).
13. C. Amra and S. Maure, "Electromagnetic power provided by sources within multilayer optics: free-space and modal patterns," J. Opt. Soc. Am. A **14**, 3102–3113 (1997).
14. C. Amra and S. Maure, "Mutual coherence and conical pattern of sources optimally excited within multilayer optics," J. Opt. Soc. Am. A **14**, 3114–3124 (1997).
15. C. Amra, "First-order vector theory of bulk scattering in optical multilayers," J. Opt. Soc. Am. A **10**, 365–374 (1993).
16. C. Amra, M. Zerrad, and M. Lequime, "Trapped light scattering within optical coatings: a multilayer roughness-coupling process," Opt. Express **29**, 25570–25592 (2021).
17. C. Amra, D. Petiteau, M. Zerrad, S. Guenneau, G. Soriano, B. Gralak, M. Bellieud, D. Veynante, and N. Rolland, "Analogies between optical propagation and heat diffusion: applications to microcavities, gratings and cloaks," Proc. R. Soc. Math. Phys. Eng. Sci. **471**, 20150143 (2015).
18. S. M. Rytov, Y. A. Kravtsov, and V. I. Tatarskii, *Principles of Statistical Radiophysics 3: Elements of Random Fields.* (Springer-Verlag, 1989).
19. L. Novotny and B. Hecht, *Principles of Nano-Optics*, 2nd ed. (Cambridge University Press, 2012).
20. Z. M. Zhang, *Nano/Microscale Heat Transfer*, 2nd ed., Mechanical Engineering Series (Springer International Publishing, 2020).
21. John R. Howell, M. Pinar Mengüç, and Robert Siegel, *Thermal Radiation Heat Transfer*, 6th ed. (CRC Press, 2016).
22. P. Rouquette, C. Amra, M. Zerrad, and C. Grèzes-Besset, "Photo-induced thermal radiation within multilayers optics," in *Advances in Optical Thin Films VII*, M. Lequime and D. Ristau, eds. (SPIE, 2021), p. 33.
23. P. Rouquette, C. Amra, M. Zerrad, C. Grèzes-Besset, and H. Krol, "Photo-induced Temperature in Optical Interference Coatings," Submitt. Opt Express (2022).
24. J.-Y. Natoli, L. Gallais, H. Akhouayri, and C. Amra, "Laser-induced damage of materials in bulk, thin-film, and liquid forms," Appl. Opt. **41**, 3156 (2002).
25. Mathias Mende, Lars O. Jensen, Henrik Ehlers, Werner Riggers, Holger Blaschke, and Detlev Ristau, "Laser-induced damage of pure and mixture material high reflectors for 355nm and 1064nm wavelength," in (Proc.SPIE, 2011), Vol. 8168.
26. L. Gallais, J. Natoli, and C. Amra, "Statistical study of single and multiple pulse laser-induced damage in glasses," Opt. Express **10**, 1465 (2002).
27. A. V. Smith and B. T. Do, "Bulk and surface laser damage of silica by picosecond and nanosecond pulses at 1064 nm," Appl. Opt. **47**, 4812–4832 (2008).
28. M. Francoeur, M. Pinar Mengüç, and R. Vaillon, "Solution of near-field thermal radiation in one-dimensional layered media using dyadic Green's functions and the scattering matrix method," J. Quant. Spectrosc. Radiat. Transf. **110**, 2002–2018 (2009).
29. L. P. Wang, S. Basu, and Z. M. Zhang, "Direct and indirect methods for calculating thermal emission from layered structures with nonuniform temperatures," J. Heat Transf. **133**, (2011).
30. P. Rouquette, C. Amra, M. Zerrad, C. Grèzes-Besset, and H. Krol, "Photo-induced Thermal Radiation in Optical Interference Coatings," Submitt. Opt. Express (2022).
31. P. Bermel, J. Lee, J. D. Joannopoulos, I. Celanovic, and M. Soljacie, "Selective solar absorbers," Annu. Rev. Heat Transf. **15**, 231–254 (2012).
32. K.-T. Lin, J. Han, K. Li, C. Guo, H. Lin, and B. Jia, "Radiative cooling: Fundamental physics, atmospheric influences, materials and structural engineering, applications and beyond," Nano Energy **80**, 105517 (2021).